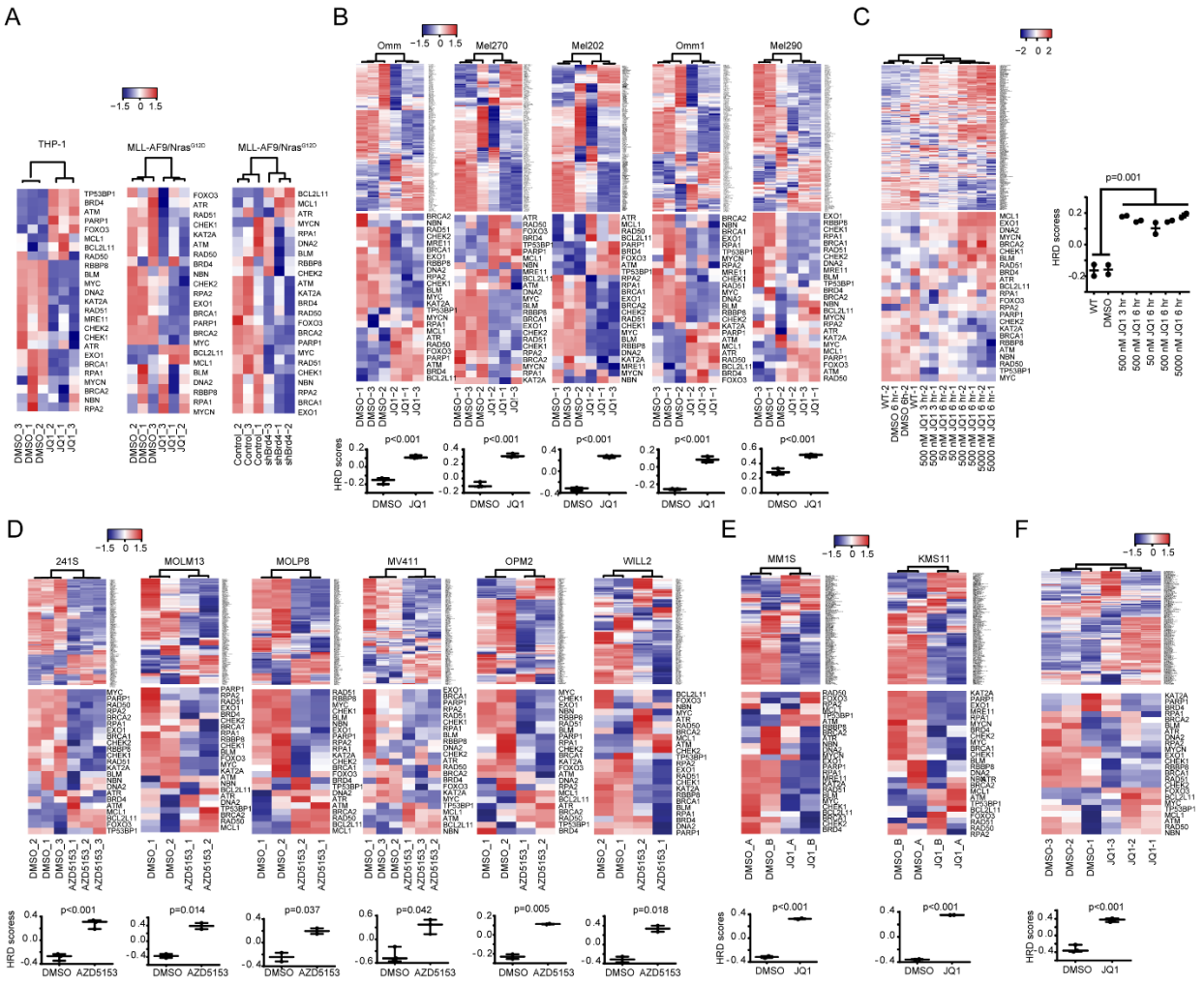

Figure S1, related to Figure 1, Effects of BRD4 inhibition on HR signature

(A) Heat maps of candidate genes after BRD4 inhibition using the GSE29799 dataset.

(B) Heat map of unsupervised clustering of HRD gene signatures (upper), candidate genes (middle), and HRD scores (lower) after treatment with 500 nM JQ1 for 24 hr in different cell lines using the GSE66048 dataset.

(C) Heat map of unsupervised clustering of HRD gene signatures (upper left), candidate genes (lower left), and HRD scores (right) after treatment with JQ1 at indicated dose or length in MM1S cells using the GSE44929 dataset.

(D) Heat map of unsupervised clustering of HRD gene signatures (upper), candidate genes (middle), and HRD scores (lower) after treatment with 200 nM AZD5153 for 24 hr in different cell lines using the GSE85840 dataset.

(E) Heat map of unsupervised clustering of HRD gene signatures (upper), candidate genes (middle), and HRD scores (lower) after treatment with 500 nM JQ1 for 24 hr in different cell lines using the GSE31365 dataset.

(F) Heat map of unsupervised clustering of HRD gene signatures (upper), candidate genes (middle), and HRD scores (lower) after treatment with 1 μM JQ1 for 24 hr in Be2C cells using the GSE43392 dataset.

Data of HRD scores after BRD4 inhibition represent mean±SEM for all panels. Statistical significances were determined using Student's t-test.

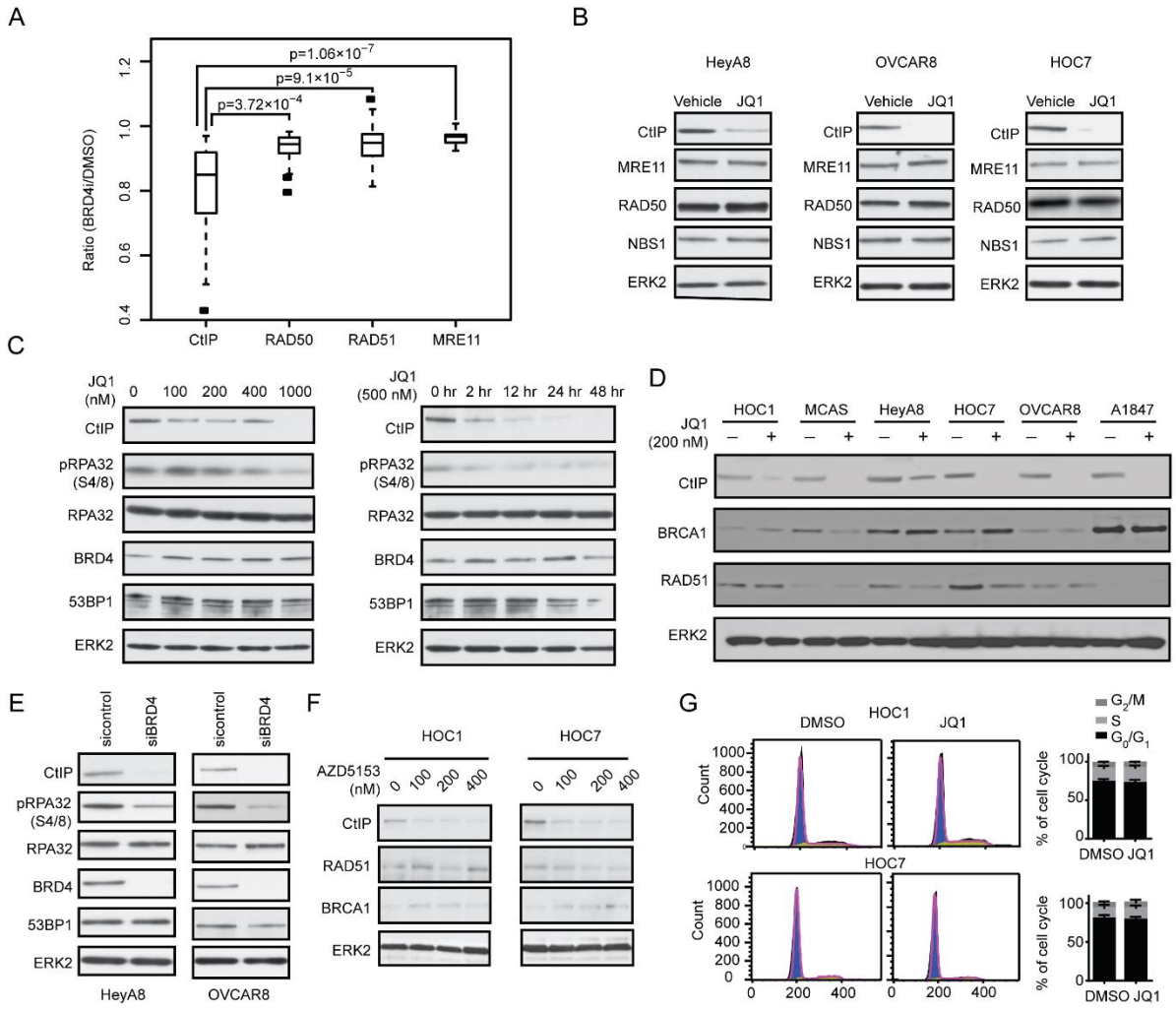

Figure S2, related to Figure 2, Effect of BRD4i on CtIP expression

(A) CtIP, RAD50, RAD51, and MRE11 proteins expression changes (BRD4i/DMSO) after treatment with BRD4i in each cell line (n = 5) from RPPA in Figure 2A. The top and bottom of the boxes indicate the 75th and 25th percentiles, respectively; line within the boxes indicates the median; lines above and below the boxes indicate the 95th and 5th percentiles, respectively. Outliers are indicated as dots. p values were calculated with Student's t test.

(B) Western blot of CtIP, MRE11, RAD50, and NBS1 after treatment with 200 nM JQ1 for 48 hr in HeyA8, OVCAR8, and HOC7 ovarian cancer cells.

(C) Western blot of indicated proteins in HeyA8 cells treated with indicated doses of JQ1 for 48 hr (left), or treated with 500 nM JQ1 for the indicated length (right).

(D) Western blot of CtIP, RAD51, and BRCA1 after treatment with 200 nM JQ1 for 48 hr in a cell line panel.

(E) Western blot of indicated proteins in HeyA8 and OVCAR8 cells after BRD4 silencing with siRNA for 48 hr.

(F) Western blot of indicated proteins in HOC1 and HOC7 cells treated with indicated doses of AZD5153 for 48 hr.

(G) Cell cycle assessment by flow cytometry (left) and quantification of percentage of cells in G_0/G_1, S, and G_2/M phase (right) in HOC1 and HOC7 cells treated with 200 nM JQ1 for 24 hr. Data represent the mean±SEM from three independent experiments.

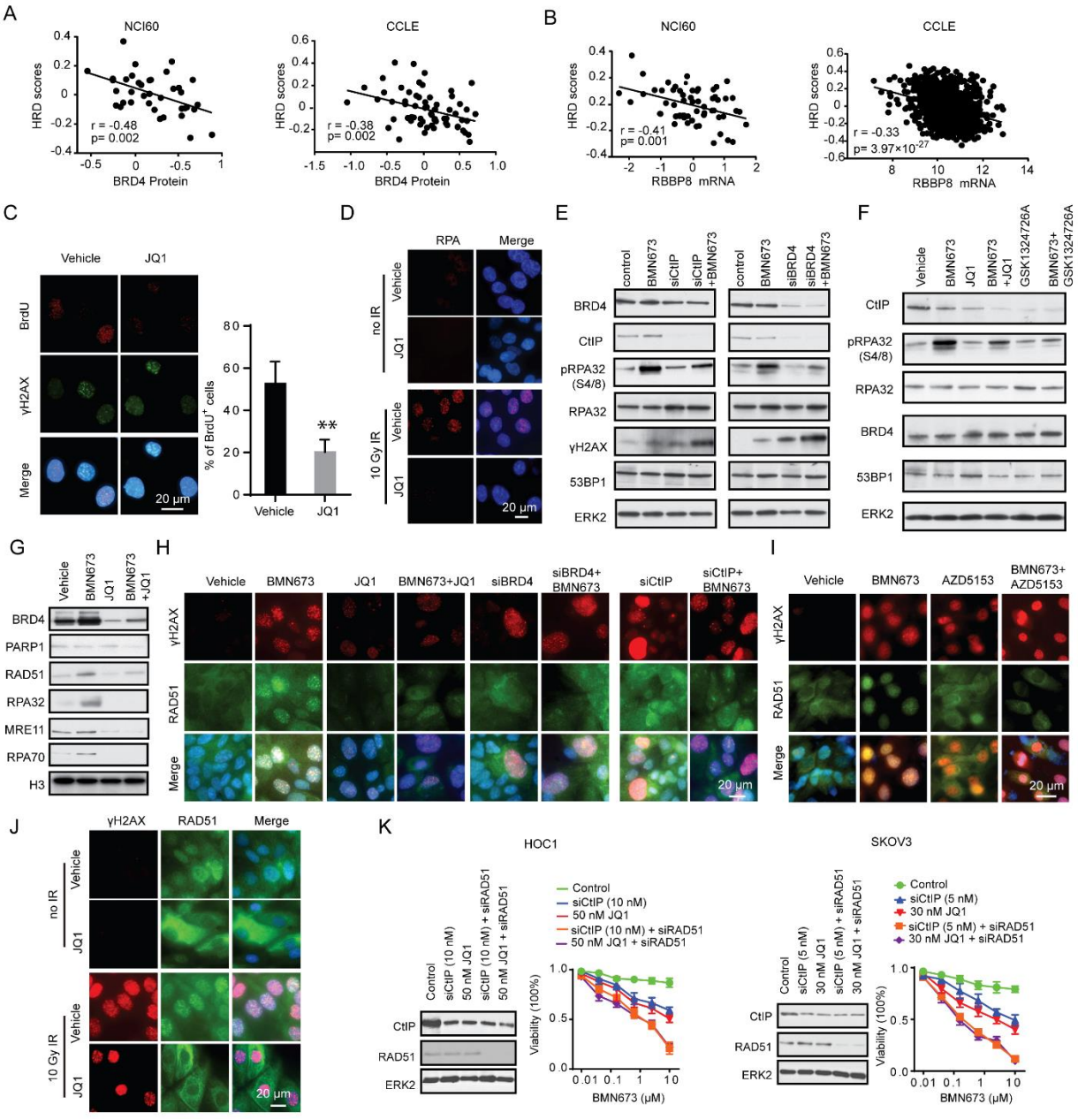

Figure S3, related to Figure 4, Effects of BRD4 inhibition on DNA end resection, generation of ssDNA, and HR function.

(A) Correlation between BRD4 protein expression and HRD scores in NCI60 and CCLE dataset.

(B) Correlation between RBBP8 mRNA expression and HRD scores in NCI60 and CCLE dataset.

(C) Representative images of BrdU and γH2AX staining under non-denaturing conditions at 4 hr after 10 Gy IR in HeyA8 cells cultured with or without 500 nM JQ1 (see STAR methods). BrdU positive cells are quantified on right. Scale bar, 20 μm.

(D) Representative images of RPA foci staining at 4 hr after 10 Gy IR in HOC1 cells with or without 200 nM JQ1. Scale bar, 20 μm.

(E) Western blot of indicated proteins in HeyA8 cells 24 hr after transfection with control, CtIP or BRD4 siRNA and then treated with 200 nM BMN673 for 48 hr.

(F) Western blot of indicated proteins in HeyA8 cells treated with BMN673 (200 nM), JQ1 (500 nM), GSK1324726A (500 nM) or the indicated combination for 48 hr.

(G) Western blot of indicated proteins in chromatin-bound fractions from HeyA8 cells treated with BMN673 (200 nM), JQ1 (500 nM), or combination for 48 hr. Histone H3 was used as a marker for chromatin-bound fraction.

(H) Representative images of RAD51 and γH2AX foci in HeyA8 cells after BRD4 inhibition (500 nM JQ1 or siRNA BRD4) for 24 hr or CtIP downregulation (siRNA CtIP) for 24 hr and then treated with 200 nM BMN673 for 48 hr. Scale bar, 20 μm.

(I) Representative images of RAD51 and γH2AX foci in HOC1 cells treated with BMN673 (200 nM), AZD5153 (200 nM), or combination for 48 hr. Scale bar, 20 μm.

(J) Representative images of RAD51 and γH2AX foci in HOC1 cells 4 hr after 10 Gy IR with or without 200 nM JQ1. Scale bar, 20 μm.

(K) Cells were transfected with indicated concentrations of CtIP siRNA or treated with indicated doses of JQ1 with or without 50 nM RAD51 siRNA for 24 hr. The dose of JQ1 and CtIP siRNA were pre-titrated to obtain similar levels of CtIP decrease. Western blots of indicated proteins are in left panel. Cells were then treated for 96 hr with indicated doses of BMN673 and viability assessed (right).

Data across panels represent mean±SEM of three independent experiments. Statistical significances were determined using Student's t-test. $^{**}p < 0.01$.

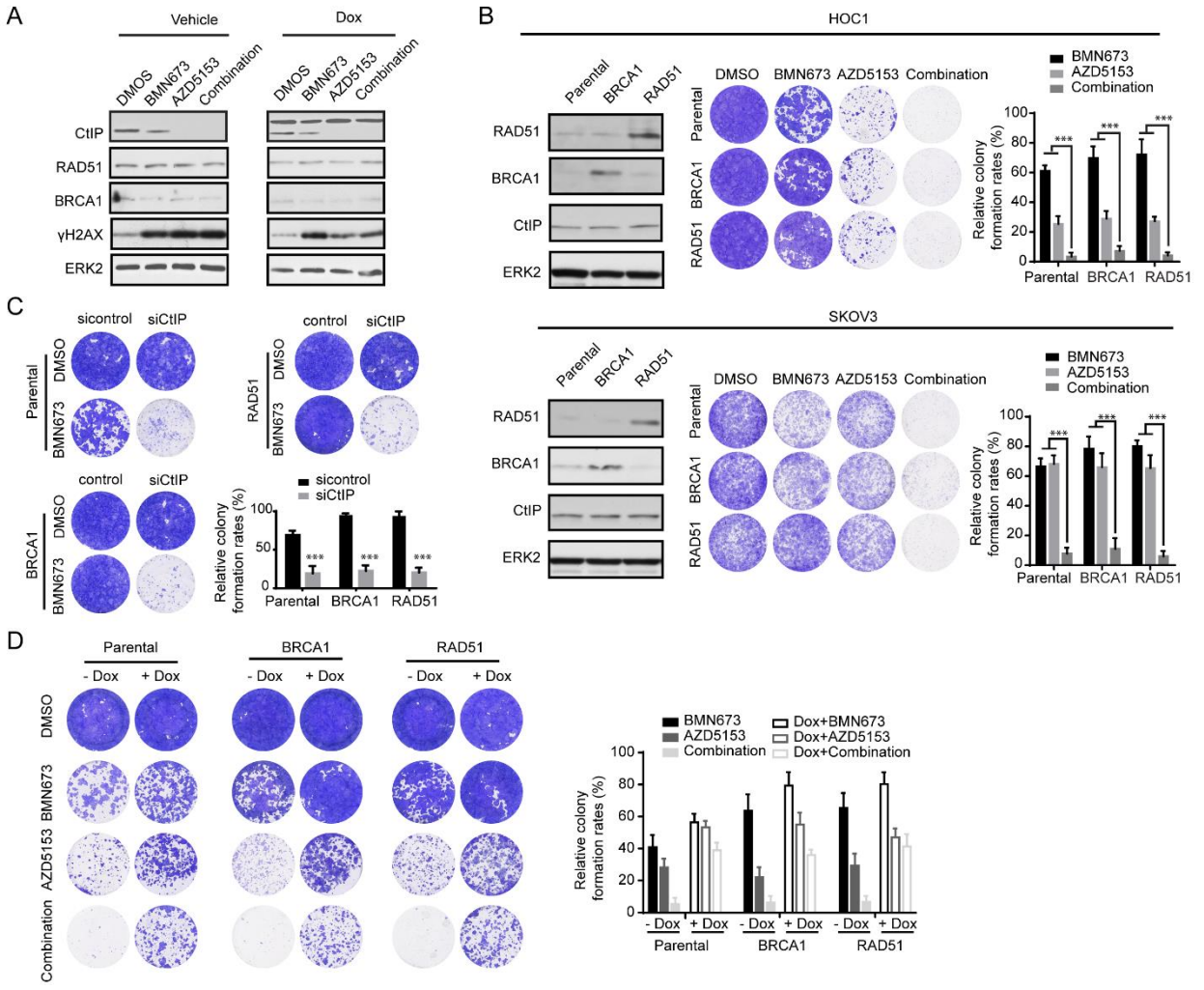

Figure S4, related to Figure 5, Effects of RAD51 and BRCA1 on synergism between BRD4i and PARPi.

(A) Western blot of indicated proteins in Dox inducible GFP-CtIP HOC1 cells treated with BMN673 (200 nM), AZD5153 (200 nM), or combination for 48 hr with or without Dox induction.

(B) Western blot of RAD51, BRCA1 and CtIP in parental HOC1 and SKOC3 cells or cells ectopically expressing RAD51 or BRCA1 are shown (left). Representative pictures (middle) and quantification (right) of clonogenic assay in parental or cells ectopically expressing RAD51 or BRCA1 treated with BMN673 (100 nM), AZD5153 (200 nM), or combination for 10 days. Colony formation rates are presented as percentage relative to DMSO.

(C) 24 hr after transfection with control, or CtIP siRNA in parental HOC1 or cells ectopically expressing RAD51 or BRCA1, clonogenic assay was performed in absence or presence of 100 nM BMN673 for 7 days. Representative pictures and quantification (lower right) of clonogenic assay are shown. Colony formation rates are presented as percentage relative to DMSO.

(D) Cells stably expressing RAD51 or BRCA1 were established in Dox inducible GFP-CtIP HOC1 cells. Representative pictures (left) and quantification (right) of clonogenic assays in parental GFP-CtIP HOC1 cells or cells

ectopically expressing RAD51 or BRCA1 treated with BMN673 (200 nM), AZD5153 (200 nM), or combination for 7 days with or without Dox induction. Colony formation rates are presented as percentage relative to DMSO.
Data across panels represent mean±SEM of three independent experiments. Statistical significances were determined using Student's t-test. ***p< 0.001.

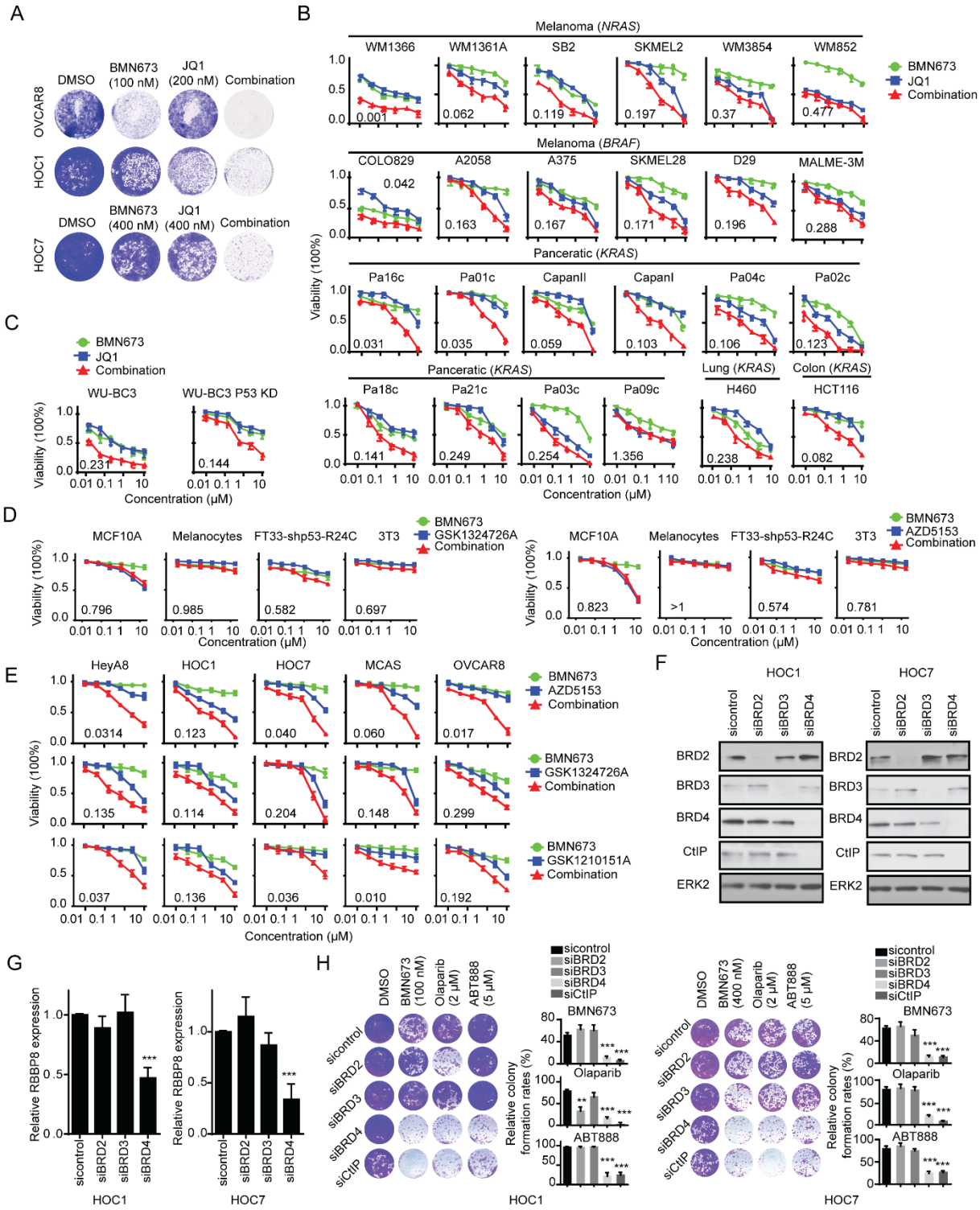

Figure S5, related to Figure 6, Effects of inhibition of different BET Bromodomain proteins on synergism between BRD4i and PARPi

(A) Representative pictures of clonogenic assay in OVCAR8, HOC1, and HOC7 cells treated with the indicated concentrations of BMN673, JQ1, or combinations for 7 days.

(B) 6 melanoma cell lines with *NRAS* mutation, 6 melanoma cell lines with *BRAF* mutation, 10 pancreatic cancer cell lines with *KRAS* mutation, 1 lung cancer cell line with *KRAS* mutation, and 1 colon cancer cell line with *KRAS* mutation were treated with varying concentrations of BMN673 or JQ1 alone or combined for 96 hr. Dose response curves are shown. CI was calculated using CalcuSyn software with the Chou-Talalay equation.

(C) Primary breast cancer cell line (WU-BC3) with or without P53 knockdown were treated with varying concentrations of BMN673 or JQ1 alone or combined for 96 hr. Dose response curves are shown.

(D) Dose response curves of BMN673 or BRD4i (GSK1324726A or AZD5153) alone or combined for 96 hr in four normal human or murine proliferating cell lines.

(E) Dose response curves of BMN673 or BRD4i (AZD5153, GSK1324726A, or GSK1210151A) alone or combined for 96 hr in five ovarian cancer cell lines.

(F) Western blot of indicated proteins in cells transfected with control, BRD2, BRD3, or BRD4 siRNA for 48 hr.

(G) qRT-PCR analysis of RBBP8 in cells transfected with control, BRD2, BRD3, or BRD4 siRNA for 48 hr.

(H) 24 hr after transfection with control, BRD2, BRD3, BRD4, or CtIP siRNA, clonogenic assay was performed in absence or presence of the indicated concentrations of BMN673, Olaparib or ABT888 for 7 days. Representative pictures (left) and quantification (right) of clonogenic assay are shown. Colony formation rates are presented as percentage relative to DMSO.Data across panels represent mean±SEM of three independent experiments. Statistical significances were determined using Student's t-test. **$p < 0.01$, ***$p < 0.001$.

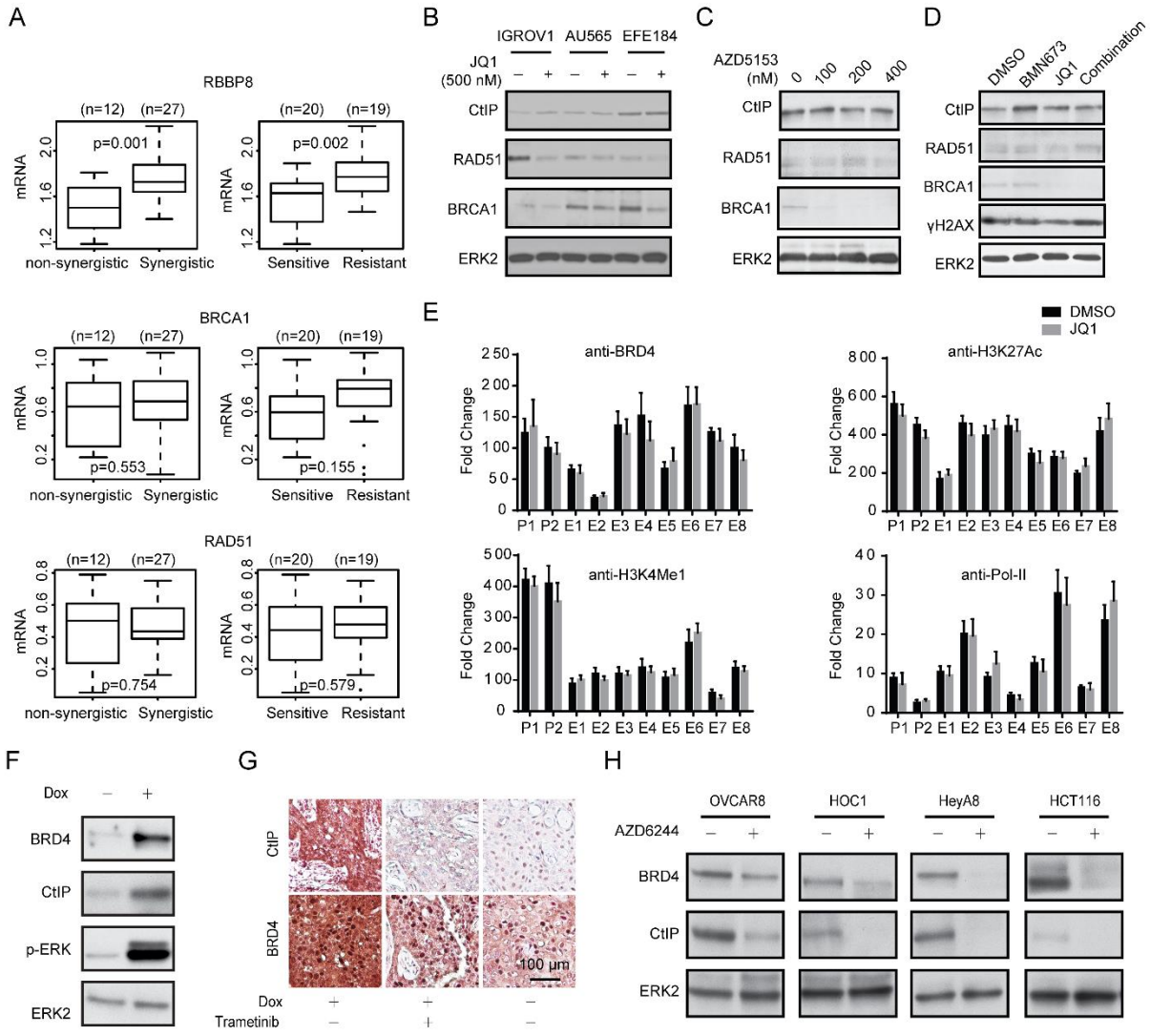

Figure S6, related to Figure 6, Association of RBBP8, RAD51 and BRCA1 mRNA levels with synergism between BRD4i and PARPi, and association of BRD4 and CtIP with *KRAS* mutations

(A) Box plot of RBBP8, RAD51 or BRCA1 mRNA levels between cells with or without synergism between BRD4i and PARPi (left) or between PARPi sensitive and resistant cells (right).The top and bottom of the boxes indicate the 75th and 25th percentiles, respectively; line within the boxes indicates the median; lines above and below the boxes indicate the 95th and 5th percentiles, respectively. Outliers are indicated as dots. p values were calculated with Student's t test.

(B) Western blot of CtIP, RAD51, and BRCA1 after treatment with 500 nM JQ1 for 48 hr in a panel of cells resistant to PARPi and BRD4i combinations.

(C) Western blot of CtIP, RAD51, and BRCA1 after treatment with indicated concentrations of AZD5153 for 48 hr in EFE184 cells.

(D) Western blot of indicated proteins after treatment with BMN673 (200 nM), JQ1 (200 nM), or combinations for 48 hr in EFE184 cells.

(E) EFE184 cells were treated with vehicle or 200 nM JQ1 for 24 hr and subjected to ChIP assay with normal rabbit IgG, BRD4, H3K27Ac, H3K4Me1 or Pol-II antibodies. ChIP samples were analyzed by qPCR using primers targeting the regions indicated in Figure 3B. Data represent mean±SEM of three independent experiments.

(F) Western blot of indicated proteins in HPDE-i*KRAS*^{G12D} cell line with or without Dox induction for 24 hr.

(G) HPDE-i*KRAS*^{G12D}cells were injected into athymic nude mice subcutaneously. Seven days after tumor injection, mice were treated with vehicle, Trametinib (2 mg/kg, oral gavage, per day) for 10 days with "Dox on" [via Dox diet (200 mg/kg; BioServ)], or "Dox off". Tumor tissues from HPDE-i*KRAS*^{G12D} xenografts were subjected to IHC and probed with indicated antibodies. Representative IHC images are shown with treatment indicated. Scale bar, 100 μm.

(H) Western blot of indicated proteins after treatment with 500 nM AZD6244 for 48 hr in four *KRAS* mutant cell lines.

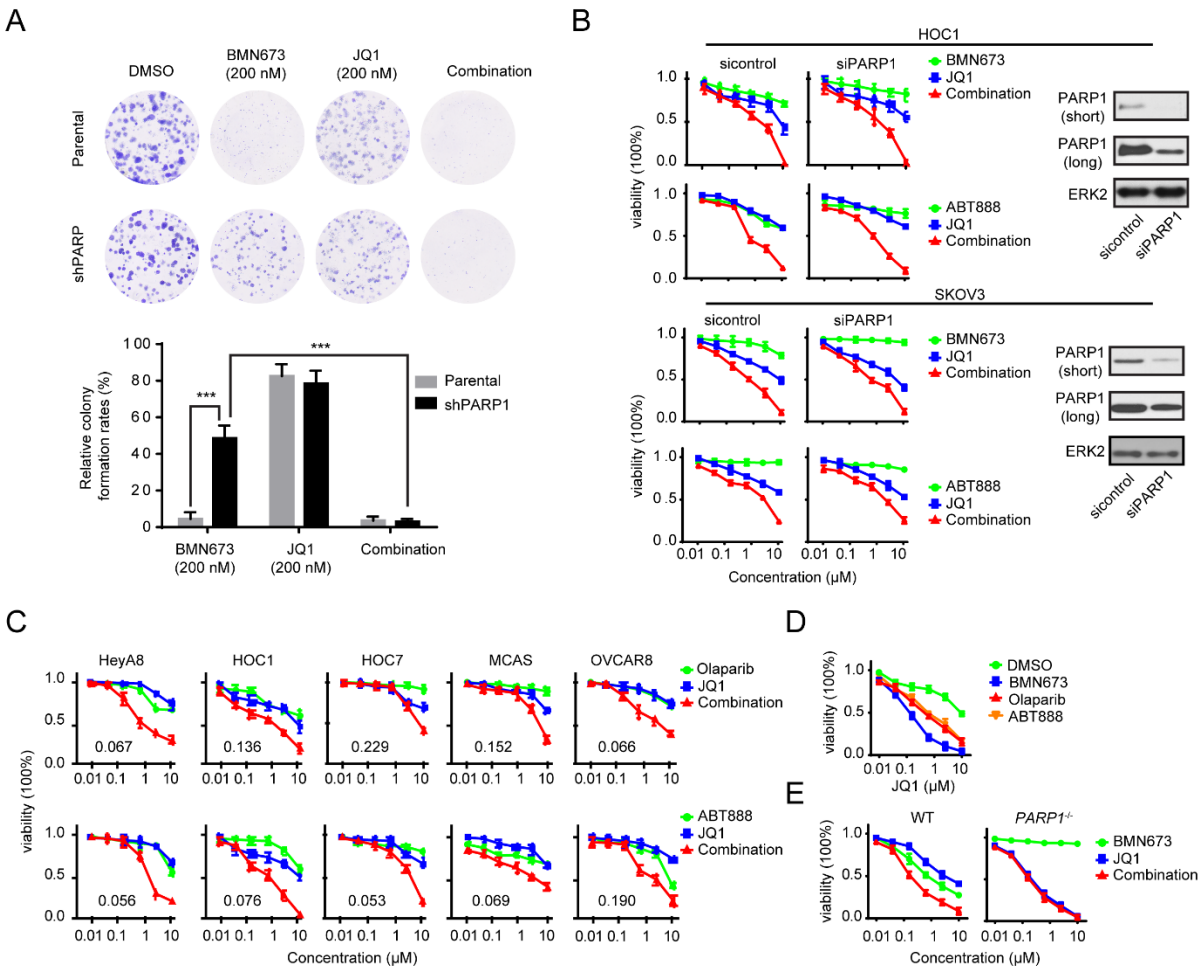

Figure S7, related to Figure 7, Effect of inhibition of PARP enzyme activity on synergy with BRD4 inhibition.

(A) Representative pictures (upper) and quantification (lower) of clonogenic assay in parental and PARP1 stable shRNA knockdown MDA-MB-231 cells treated with the indicated concentrations of BMN673, JQ1, or combination for 7 days. Colony formation rates are presented as percentage relative to DMSO.

(B) 24 hr after transfection with control, or PARP1 siRNA, cells were treated with varying concentrations of JQ1 or PARPi (BMN673 or ABT888) alone or combined for 96 hr. Dose response curves (left) and Western blots of PARP1 in cells transfected with control or PARP1 siRNA for 24 hr (right) are shown. Short: short time exposure, long: long time exposure.

(C) Dose response curves of PARPi (Olaparib, or ABT888) or JQ1 alone or combined for 96 hr in five ovarian cancer cell lines. CI was calculated using CalcuSyn software with the Chou-Talalay equation.

(D) Dose response curves of JQ1 alone or combined with BMN673 (500 nM), Olaparib (2 μM), or ABT888 (5 μM) for 96 hr in HOC1 cells.

(E) Dose response curves of BMN673 or JQ1 alone or combined for 96 hr in DT40 WT or DT40 *PAPR1*$^{-/-}$ cells.

Data represent mean±SEM of three independent experiments. Statistical significances were determined using Student's t-test. ***p< 0.001.

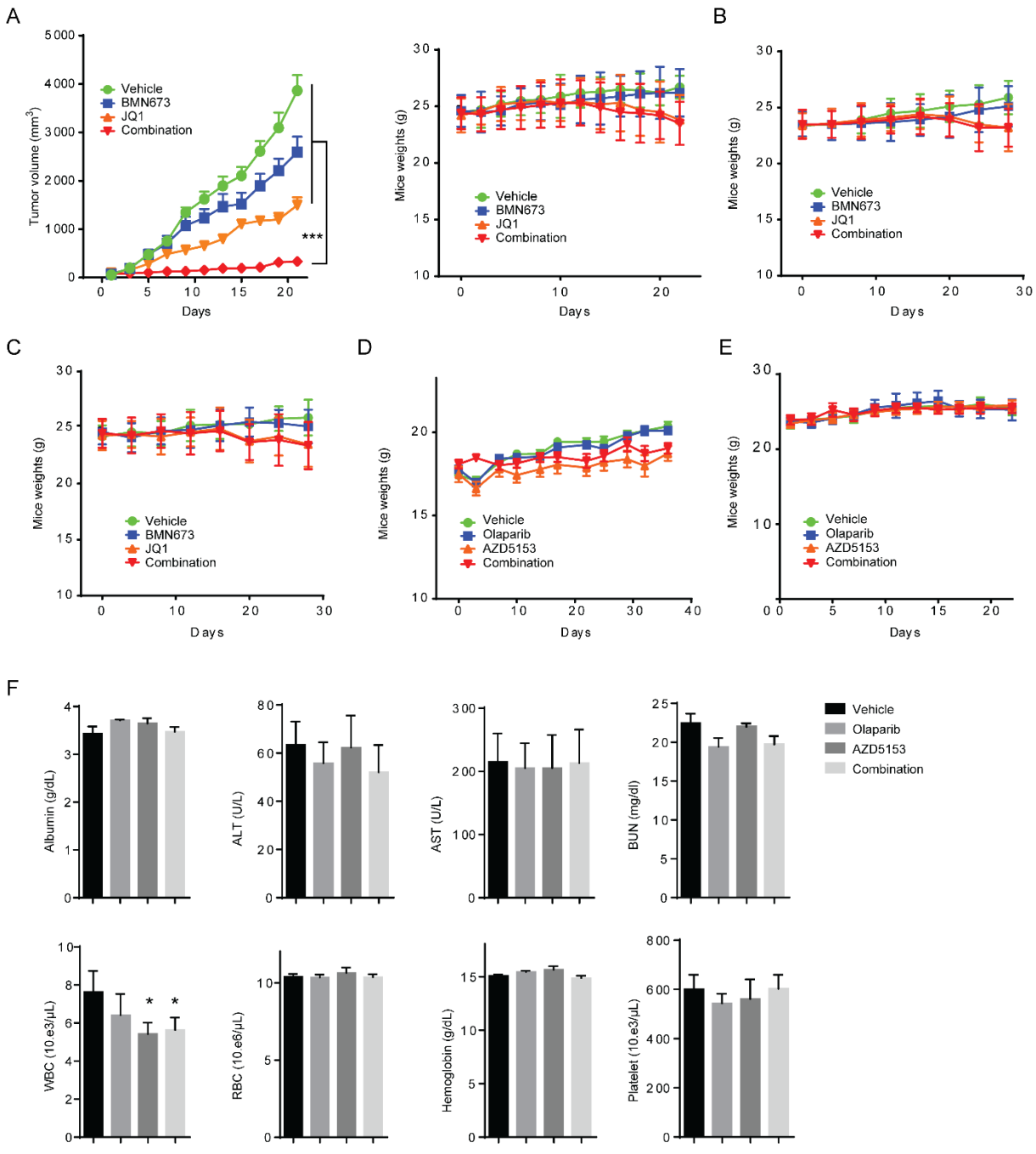

Figure S8, related to Figure 8, Toxicity of PARPi, BRD4i and combination therapy *in vivo*.

(A) LPA1-T127 tumor tissues were transplanted into the mammary fat pads of FVB mice. Eight days later, mice were randomized into treatment cohorts: vehicle (0.5% hydroxypropylmethylcellulose and 0.2% Tween 80), BMN673 (0.333 mg/kg, oral gavage, per day), JQ1 (40 mg/kg, I.P., per day), or combination of BMN673 and JQ1 (n = 6 for each group). Tumor volume curves (left) and body weight curves of mice (right) are shown. Analysis of variance (ANOVA) was used for statistical significance. ***p< 0.001.

(B) Body weight curves of mice with OVCAR8 xenografts treated with vehicle (0.5% hydroxypropylmethylcellulose and 0.2% Tween 80), BMN673 (0.333 mg/kg, oral gavage, per day), JQ1 (40 mg/kg, I.P., per day), or combination of BMN673 and JQ1.

(C) Body weight curves of mice with WU-BC3 PDX treated with vehicle (0.5% hydroxypropylmethylcellulose and 0.2% Tween 80), BMN673 (0.333 mg/kg, oral gavage, per day), JQ1 (40 mg/kg, I.P., per day), or combination of BMN673 and JQ1.

(D) Body weight curves of mice with OVCAR3 xenograft treated with vehicle (0.5% hydroxypropylmethylcellulose and 0.2% Tween 80), Olaparib (100 mg/kg, oral gavage, per day), AZD5153 (2.5 mg/kg, oral gavage, per day), or combination of Olaparib and AZD5153.

(E) Body weight curves of mice with LPA1-T127 allograft treated with vehicle (0.5% hydroxypropylmethylcellulose and 0.2% Tween 80), Olaparib (100 mg/kg, oral gavage, per day), AZD5153 (2.5 mg/kg, oral gavage, per day), or combination of Olaparib and AZD5153.

(F) Plot of Albumin, ALT, AST, BUN, White blood cell (WBC), Red blood cell (RBC), Platelet count, and Hemoglobin levels in mice with LPA1-T127 allograft treated with vehicle, Olaparib (100 mg/kg, oral gavage, per day), AZD5153 (2.5 mg/kg, oral gavage, per day), or combination of Olaparib and AZD5153 ($n = 6$ mice in each group). Statistical significances were determined using Student's t-test. $*p < 0.05$.

Data are presented as mean ± SEM across all panels.

Table S1, related to STAR methods, Information about cell lines used in this paper.

Cell lines	Species	Gender	Culture Media	Source	Identifier
A1847	human	female	RPMI-1640+10% FBS+Insulin	MDACC characterized Cell line Core	N/A
A2780	human	female	RPMI-1640+5% FBS	MDACC characterized Cell line Core	N/A
A2780CP	human	female	RPMI-1640+5% FBS	MDACC characterized Cell line Core	N/A
ARK1	human	female	RPMI-1640+10% FBS	MDACC characterized Cell line Core	N/A
ARK2	human	female	RPMI-1640+10% FBS	MDACC characterized Cell line Core	N/A
AU565	human	female	RPMI-1640+10% FBS	MDACC characterized Cell line Core	N/A
BT20	human	female	RPMI-1640+10% FBS	MDACC characterized Cell line Core	N/A
BT474	human	female	RPMI-1640+10% FBS	MDACC characterized Cell line Core	N/A
BT549	human	female	RPMI-1640+5% FBS	MDACC characterized Cell line Core	N/A
CAOV3	human	female	RPMI-1640+20% FBS	MDACC characterized Cell line Core	N/A
ECC1	human	female	RPMI-1640+10% FBS	MDACC characterized Cell line Core	N/A
EF027	human	female	RPMI-1640+10% FBS	MDACC characterized Cell line Core	N/A
EFE184	human	female	RPMI-1640+10% FBS	MDACC characterized Cell line Core	N/A
EI	human	female	DMEM+10% FBS	MDACC characterized Cell line Core	N/A
ENT1	human	female	RPMI-1640+10% FBS	MDACC characterized Cell line Core	N/A
ES2	human	female	McCoy's 5a +10% FBS	MDACC characterized Cell line Core	N/A
HAC2	human	female	DMEM/F12+10% FBS	MDACC characterized Cell line Core	N/A
HCC1187	human	female	RPMI-1640+10% FBS	MDACC characterized Cell line Core	N/A
HCC1500	human	female	RPMI-1640+10% FBS	MDACC characterized Cell line Core	N/A
HCC1937	human	female	RPMI-1640+10% FBS	MDACC characterized Cell line Core	N/A
HCC1954	human	female	RPMI-1640+10% FBS	MDACC characterized Cell line Core	N/A
HCC70	human	female	RPMI-1640+10% FBS	MDACC characterized Cell line Core	N/A
HEC108	human	female	RPMI-1640+10% FBS	MDACC characterized Cell line Core	N/A
HEC116	human	female	DMEM+10% FBS	MDACC characterized Cell line Core	N/A
HEC151	human	female	RPMI-1640+10% FBS	MDACC characterized Cell line Core	N/A
HEC1A	human	female	McCoy's 5a +10% FBS	MDACC characterized Cell line Core	N/A
HEC1B	human	female	McCoy's 5a +10% FBS	MDACC characterized Cell line Core	N/A
HEC251	human	female	RPMI-1640+10% FBS	MDACC characterized Cell line Core	N/A
HeyA8	human	female	RPMI-1640+10% FBS	MDACC characterized Cell line Core	N/A
HOC1	human	female	RPMI-1640+5% FBS	MDACC characterized Cell line Core	N/A
HOC7	human	female	RPMI-1640+5% FBS	MDACC characterized Cell line Core	N/A
HOC8	human	female	RPMI-1640+5% FBS	MDACC characterized Cell line Core	N/A
IGROV1	human	female	RPMI-1640+10% FBS	MDACC characterized Cell line Core	N/A

KK	human	female	RPMI-1640+10% FBS	MDACC characterized Cell line Core	N/A
KLE	human	female	RPMI-1640+10% FBS	MDACC characterized Cell line Core	N/A
MCAS	human	female	RPMI-1640+10% FBS	MDACC characterized Cell line Core	N/A
MCF7	human	female	RPMI-1640+5% FBS	MDACC characterized Cell line Core	N/A
MCF10A	human	female	Special Medium (ATCC Webpage)	MDACC characterized Cell line Core	N/A
MDA-MB-231	human	female	RPMI-1640+5% FBS	MDACC characterized Cell line Core	N/A
MDA-MB-436	human	female	DMEM+10% FBS	MDACC characterized Cell line Core	N/A
MDA-MB-468	human	female	DMEM/F12+10% FBS	MDACC characterized Cell line Core	N/A
MFE296	human	female	RPMI-1640+20% FBS+Insulin	MDACC characterized Cell line Core	N/A
MFE319	human	female	RPMI-1640+10% FBS	MDACC characterized Cell line Core	N/A
OAW42	human	female	RPMI-1640+5% FBS	MDACC characterized Cell line Core	N/A
OC316	human	female	RPMI-1640+5% FBS	MDACC characterized Cell line Core	N/A
OVCAR3	human	female	RPMI-1640+5% FBS	MDACC characterized Cell line Core	N/A
OVCAR4	human	female	RPMI-1640+5% FBS	MDACC characterized Cell line Core	N/A
OVCAR5	human	female	RPMI-1640+5% FBS	MDACC characterized Cell line Core	N/A
OVCAR8	human	female	RPMI-1640+10% FBS	MDACC characterized Cell line Core	N/A
PANC1	human	female	DMEM+10% FBS	MDACC characterized Cell line Core	N/A
PEO-1	human	female	RPMI-1640+5% FBS	MDACC characterized Cell line Core	N/A
SKBR3	human	female	RPMI-1640+20% FBS	MDACC characterized Cell line Core	N/A
SKOV3	human	female	RPMI-1640+5% FBS	MDACC characterized Cell line Core	N/A
T47D	human	female	RPMI-1640+5% FBS	MDACC characterized Cell line Core	N/A
TOV21G	human	female	1:1 Medium 199/MCDB105+15% FBS	MDACC characterized Cell line Core	N/A
UWB1.289	human	female	RPMI-1640:MEGM+3% FBS	MDACC characterized Cell line Core	N/A
UWB1.289-BRCA1	human	female	RPMI-1640:MEGM+3% FBS	MDACC characterized Cell line Core	N/A
Pa01C	human	N/A	RPMI-1640+10% FBS	Laboratory of Dr. Anirban Maitra	N/A
Pa02C	human	N/A	RPMI-1640+10% FBS	Laboratory of Dr. Anirban Maitra	N/A
Pa03C	human	N/A	RPMI-1640+10% FBS	Laboratory of Dr. Anirban Maitra	N/A
Pa04C	human	N/A	RPMI-1640+10% FBS	Laboratory of Dr. Anirban Maitra	N/A
Pa09C	human	N/A	RPMI-1640+10% FBS	Laboratory of Dr. Anirban Maitra	N/A
Pa16C	human	N/A	RPMI-1640+10% FBS	Laboratory of Dr. Anirban Maitra	N/A
Pa18C	human	N/A	RPMI-1640+10% FBS	Laboratory of Dr. Anirban Maitra	N/A
Pa21C	human	N/A	RPMI-1640+10% FBS	Laboratory of Dr. Anirban Maitra	N/A

CAPAN Ⅰ	human	male	RPMI-1640+10% FBS	MDACC characterized Cell line Core	N/A
CAPAN Ⅱ	human	male	RPMI-1640+10% FBS	MDACC characterized Cell line Core	N/A
WM1366	human	male	RPMI-1640+10% FBS	MDACC characterized Cell line Core	N/A
WM1361A	human	N/A	RPMI-1640+10% FBS	MDACC characterized Cell line Core	N/A
SB2	human	N/A	RPMI-1640+10% FBS	MDACC characterized Cell line Core	N/A
SKMEL2	human	male	RPMI-1640+10% FBS	MDACC characterized Cell line Core	N/A
WM3854	human	male	DMEM+10% FBS	MDACC characterized Cell line Core	N/A
WM852	human	male	DMEM+10% FBS	MDACC characterized Cell line Core	N/A
COLO829	human	male	DMEM+10% FBS	MDACC characterized Cell line Core	N/A
A2058	human	male	DMEM+10% FBS	MDACC characterized Cell line Core	N/A
A375	human	female	DMEM+10% FBS	MDACC characterized Cell line Core	N/A
SKMEL28	human	male	RPMI-1640+10% FBS	MDACC characterized Cell line Core	N/A
D29	human	N/A	RPMI-1640+10% FBS	MDACC characterized Cell line Core	N/A
MALME-3M	human	male	RPMI-1640+10% FBS	MDACC characterized Cell line Core	N/A
H460	human	male	DMEM+10% FBS	MDACC characterized Cell line Core	N/A
HCT116	human	male	RPMI-1640+5% FBS	MDACC characterized Cell line Core	N/A
WU-BC3	human	female	DMEM/F12+10% FBS	Laboratory of Dr. Helen Piwnica-Worms	N/A
WU-BC3 P53 KD	human	female	DMEM/F12+10% FBS	Laboratory of Dr. Helen Piwnica-Worms	N/A
MDA-MB-231	human	female	RPMI-1640+5% FBS	Laboratory of Dr. Mien-Chie Hung	N/A
MDA-MB-231 PARP1 KD	human	female	RPMI-1640+5% FBS	Laboratory of Dr. Mien-Chie Hung	N/A
Melanocytes	human	N/A	Special Medium (Look up on ATCC Webpage)	ATCC	PCS-200-013
FT33-shp53-R24C	human	female	WIT+15% FBS	ABM	T0609
3T3	mouse	N/A	DMEM+10% FBS	MDACC characterized Cell line Core	N/A
DT40	chicken	N/A	RPMI-1640+10% FBS+5% Chicken serum	Laboratory of Dr. Shunichi Takeda	N/A
DT40 *PARP1*$^{-/-}$	chicken	N/A	RPMI-1640+10% FBS+5%Chicken serum	Laboratory of Dr. Shunichi Takeda	N/A
HPDE-i*KRAS*^{G12D}	human	N/A	KSFM	Laboratory of Dr. Kenneth L. Scott	N/A
U2OS DR-GFP	human	female	McCoy's 5a +10% FBS	MDACC characterized Cell line Core	N/A

Table S2, related to STAR methods, Information of Oligonucleotides used in this paper.

Purpose	Name	Source	Identifier	Sequence
ChIP-qPCR	P1-Forward	Sigma	N/A	ATTGTCGTCGTGCCTCGAAT
	P1-Reverse	Sigma	N/A	AAACCCTTTCCACCTACCCG
	P2-Forward	Sigma	N/A	CACCCAGGCAAATGTTTGGTC
	P2-Reverse	Sigma	N/A	GCTTAGCCTTGAGGAGCGAG
	E1-Forward	Sigma	N/A	CTGTTGCTGAGCTACCAAGGA
	E1- Reverse	Sigma	N/A	TCATCAGGCAACCAAGCCAT
	E2-Forward	Sigma	N/A	GTGGCTCCCTACACCAAACA
	E2-Reverse	Sigma	N/A	GCCAGAAGCCCAGTGGTAAT
	E3-Forward	Sigma	N/A	ATTATGTCGCCGGAACTGGT
	E3-Reverse	Sigma	N/A	AGACCGAGGAAGACCTGACT
	E4-Forward	Sigma	N/A	TGGTTCCCCAGTTCTGTTGG
	E4-Reverse	Sigma	N/A	CCTGGACATGTCTGGAAAGTGA
	E5-Forward	Sigma	N/A	TTACCAGCTTACAGACTCCTGC
	E5-Reverse	Sigma	N/A	TGTGGGAGTTCCCTGAGTCTAA
	E6-Forward	Sigma	N/A	CATGCCAACACCCGCTCATA
	E6-Reverse	Sigma	N/A	CCCCAACGGGGTTGTCAAAA
	E7-Forward	Sigma	N/A	CACACAAGCCAGCTTTTACTGT
	E7-Reverse	Sigma	N/A	ACTTGGTAGGGGCACATTGG
	E8-Forward	Sigma	N/A	AAAATGTTCTCCCGCCAGCA
	E8-Reverse	Sigma	N/A	CAAGCATGCCCAGTGTTTGC
qRT-PCR	cMYC-Forward	Sigma	N/A	CAGCGACTCTGAGGAGGAAC
	cMYC-Reverse	Sigma	N/A	GCTGGTGCATTTTCGGTTGT
	RBBP8-Forward	Sigma	N/A	GGCTTATGTGATCGCTGTGC
	RBBP8-Reverse	Sigma	N/A	ATGTGCTTTGGCCATTGGAG
Site-directed mutagenesis	CtIP_T847A_F	Sigma	N/A	TTCCGCTACATTCCACCCAACGC TCCAGAGAATTTTTGGGAAGTT
	CtIP_T847A_R	Sigma	N/A	AACTTCCCAAAAATTCTCTGGAG CGTTGGGTGGAATGTAGCGGAA
siRNA	CtIP siRNA	GE Dharmacon	L-011376-00-0005	N/A
	BRD4 siRNA	GE Dharmacon	L-004937-00-0005	N/A
	53BP1 siRNA	GE Dharmacon	L-003548-00-0005	N/A
	PARP1 siRNA	GE Dharmacon	L-006656-03-0005	N/A
	BRD2 siRNA	GE Dharmacon	L-004935-00-0005	N/A
	BRD3 siRNA	GE Dharmacon	L-004936-00-0005	N/A
	ON-TARGETplus Non-targeting Pool	GE Dharmacon	D-001810-10-05	N/A